DEVELOPMENT AND PERFORMANCE EVALUATION OF A NOVEL PEELING DEVICE FOR HIGH-MOISTURE CORN COBS

/

高含水率玉米果穗剥皮装置设计与试验

Bang JI [1,3], Long PAN [1], Yusong XIE [1], Hao ZHOU [1], Yongkang LI [1], Pu LI [*2]
[1] Hunan Agricultural University, College of Mechanical and Electrical Engineering, Changsha/China;
[2] Hunan Mechanical and Electrical Polytechnic, Changsha/China;
[3] Hunan Key Laboratory of Intelligent Agricultural Machinery and Equipment, Changsha/China.
Tel: +86 17375860294; E-mail: 619741039@qq.com
Corresponding author: Pu Li
DOI: https://doi.org/10.35633/inmateh-75-82

Keywords: *corn peeling, high-moisture corn cobs, high-speed camera, scratching device, friction peeling*

ABSTRACT

To address the challenges of high moisture content and the difficulty of peeling corn cobs in certain regions during harvest, a novel peeling device was developed. The device uses directional friction to peel the cob after introducing scratches on the bracts. Mechanical and kinematic analyses were conducted to study the peeling process, along with the design of the scratching mechanism. High-speed camera technology was employed to observe the peeling process, confirming that the peeling rollers effectively gripped the bracts at the scratched points. A three-factor, three-level response surface optimization experiment was carried out, using peeling roller speed, pressing wheel speed, and the distance between the pressing wheel and the peeling roller as independent variables, with bract peeling rate and grain shedding rate as the response indicators. The results showed that at a peeling roller speed of 353.2 r·min^{-1}, a pressing wheel speed of 81.42 r·min^{-1}, and a distance of 37.16 mm between the pressing wheel and the peeling roller, the bract peeling rate reached 95.67% with a grain shedding rate of 1.45%. Validation tests under these conditions yielded a bract peeling rate of 93.33% and a grain shedding rate of 1.56%, meeting the operational requirements for efficient corn peeling.

摘要

针对部分地区大田玉米在收获时其含水率高剥皮困难等问题，设计了一款在果穗苞叶上划痕后定向摩擦去皮的剥皮装置。对果穗剥皮过程进行力学与运动学分析，并对划痕装置进行设计。采用高速摄像技术对果穗剥皮过程进行研究并验证了剥皮辊在苞叶划痕处能有效的抓取到苞叶。以剥皮辊转速、压送器转速和压送器距剥皮辊间距作为试验因素，以苞叶剥净率和籽粒损失率作为试验指标，进行三因素三水平响应曲面优化试验。结果表明: 当剥皮辊转速为 353.2 r·min^{-1}、压送器转速为 81.42 r·min^{-1}、压送器距剥皮辊间距为 37.16mm 时，此时苞叶剥净率为 95.67%，籽粒损失率为 1.45%。在该条件下开展验证试验，得到苞叶剥净率、籽粒损失率分别为 93.33%、1.56%，满足玉米剥皮要求。

INTRODUCTION

In some regions, the high moisture content of corn cobs at maturity, generally ranging from 30% to 40%, is primarily due to the local climate and environmental conditions *(Chen et al., 2014; Li et al., 2024)*. As a result, directly harvesting kernels often leads to a higher kernel breakage rate. Consequently, the standard method involves harvesting the entire cob, followed by drying, peeling, and threshing *(Chen et al., 2023)*. Given the high moisture content at harvest, if the cobs are not dried and peeled promptly, they are prone to deterioration and germination, which significantly affects their value *(Zhao et al., 2024; Barnwal et al., 2012)*. Therefore, the development of an efficient method for peeling corn cobs with high moisture content is of paramount importance.

In recent years, numerous scholars have focused on improving the material properties of corn cobs and optimizing the structure of key components involved in the peeling process, to enhance the operational efficiency of peeling devices *(Xie et al., 2018; Liu et al., 2020)*. *Plett et al. (1994)* conducted a study on various corn cob varieties to assess kernel crushing and found that the lowest kernel crushing rate occurred when the moisture content was between 16.7% and 22.1%.

Bang Ji, Lect. Ph.D.; Long Pan, M.S. Stud.;Yusong Xie, M.S. Stud.; Hao Zhou, M.S. Stud.; Yongkang Li, M.S. Stud; Pu Li, Lect. M.S.

Li Zhenye et al. (2021) investigated the physical and tensile properties of corn cob bracts throughout the harvest period, developing a mathematical model that correlates bract tensile properties with moisture content and thickness.

Liu Lei et al. (2022) established a discrete element method (DEM)-based simulation model to analyze the corn peeling process, focusing on kernel crushing and shedding. Their study provided insights into the cob peeling process and highlighted the extent of kernel damage to light cobs during interaction with the peeling roller. The Kubota PRO1408Y-4 self-propelled corn cob harvester, produced by Kubota Agricultural Machinery Co., Ltd. in Japan, features an extended peeling roller (1.1 m in length), which ensures a high peeling rate even at elevated speeds. Additionally, the spacing between the pressing wheel and the peeling roller can be adjusted via a handle, allowing the device to accommodate different corn cob sizes *(Shirly., 2015)*. Although these studies demonstrate effective peeling performance at low moisture content, they are less suited for high-moisture corn cobs. When corn cobs have high moisture content, the bracts and kernels bond more tightly, which prevents the peeling rollers from effectively gripping the bracts and performing an efficient peeling operation.

To address these challenges, the present study designs a peeling device specifically for the directional friction peeling of corn cob bracts after initial scratching. This design is based on an analysis of the physical properties and peeling requirements of the bracts from high-moisture corn cobs. Through theoretical analysis of the peeling process and the design of key components, the study also employs high-speed camera technology to verify that the peeling rollers can effectively grip and peel the bracts. Finally, through bench testing, relevant parameters are optimized to facilitate the efficient peeling of high-moisture corn cobs.

MATERIALS AND METHODS

Machine structure and working principle

The high-moisture-content corn cob peeling device consists of two main components: the scratching device and the peeling device, as illustrated in Fig. 1. During operation, the cob initially passes through the scratching device, where it is guided along a semi-circular rail. The rail is situated below the blade. As the cob progresses along the guide rail, it passes beneath the blade, which creates scratches on the bracts. Following this, the cob enters the peeling device. The rollers continuously grasp the bracts at the locations of the scratches *(Zhao et al., 2012)*.

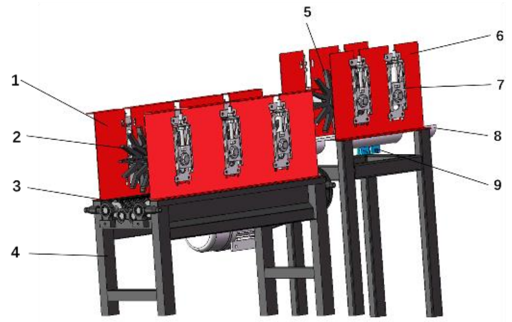

Fig. 1 – Three-dimensional structure of corn cob peeling device

1 - Peeling device; 2 - Pressing wheel; 3 - Peeling roller; 4 - Frames; 5 - Pressing wheels; 6 - Scratching devices; 7 - Height-adjustable bearing seats; 8 - Semi-circular guide rail; 9 - Knife holders.

Modeling of corn cob-mechanics

Cob bracts scratch force analysis

In the semicircular guide scratching process, the force conditions are illustrated in Fig. 2.

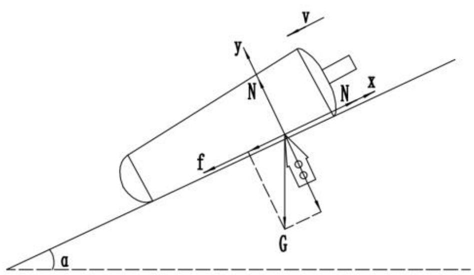

Fig. 2 – Force analysis diagram for cob bracts scratching process

When the cob is fed into the scratching device, it moves downward along the guide rail with a specified acceleration α, and the blade scratches the cob bracts under the action of the pressing force F. The force equation of the scratching process is given in Eq. (1) and (2).

$$mg\ sin\alpha+f\text{-}F=ma \tag{1}$$

$$\begin{cases} N=mg\ cos\alpha \\ f=\mu_1\ N\ F \end{cases} \tag{2}$$

From Equations 1 and 2, will result:

$$a=g\left(sin\alpha+\mu_1 cos\alpha\right)-\frac{2F}{m} \tag{3}$$

where:

m is the unpeeled cob mass, [kg]; g is the acceleration due to gravity, [m·s^{-2}]; f is the frictional resistance of the guide rail acting on the cob, [N]; N is the support force of the guide rail on the cob, [N]; μ_1 is the friction factor between the guide rail and the cob; α is the guide rail inclination angle, [°].

When the Corn cob moves within the guide rail at a uniform linear velocity, then:

$$S=v_0t+\frac{1}{2}at^2 \tag{4}$$

where:

S is the length of the guide rail, [m]; V_0 is the initial feeding speed of the corn cob [m·s^{-1}]; t is the cob peeling time, [s].

Substituting Eq. (3) into Eq. (4), the required force F for cob scratching is obtained, as shown in Eq. (5).

$$F=\frac{m\left[gt^2\left(sin\alpha+\mu_1 cos\alpha\right)\text{-}2\left(S\text{-}v_0t\right)\right]}{2t^2} \tag{5}$$

Equation (5) shows that the scratching process is influenced by the inclination angle of the guide rail, α. Based on the peeling device's inclination angle, the value of α can range from 10° to 20°.

Conditions required for cob bracts peeling

As shown in Fig. 3, consider the peeling process of the bracts from point A to point B. The length of the bract from point A to point B is denoted as C. Treating the bract as an elastomer, a mechanical model for bract peeling is established to study the peeling process. During the bract peeling process, the action of the peeling force F on the bracts can be divided into three distinct components *(Rivlin et al., 1997; Kendall et al., 1975)*.

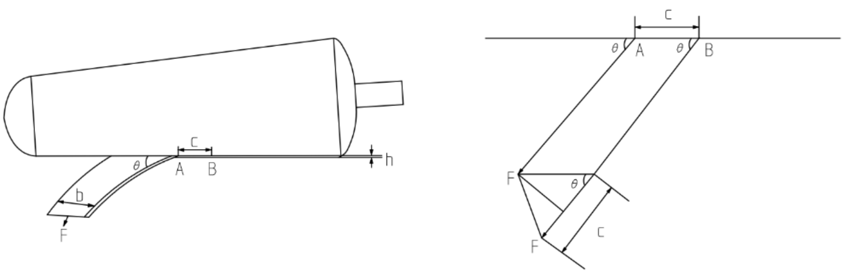

Fig. 3 – Schematic diagram of bracts peeling

Surface energy W_s refers to the energy generated when the peeling force F peels the upper bracts from the lower bracts as seen in Eq. (6):

$$W_s=\text{-}b\ c\ R \tag{6}$$

Potential energy W_p denotes the energy generated by the movement of the peeling force F from point A to point B as seen in Eq. (7):

$$W_p = c(1-\cos\theta)F \tag{7}$$

Elastic potential energy: W_e refer to the energy produced by the peeling force F as it stretches the bracts. This energy comprises two components:

The first component is the work W_{e1} done by the constant force F in the stretching region:

$$W_e = F\triangle c \tag{8}$$

It is known that $E = \frac{F/_{bh}}{\triangle c/_c}$, $\triangle c = \frac{Fc}{E\,b\,h}$, thus:

$$W_{e1} = \frac{F^2 c}{E\,b\,h} \tag{9}$$

The second component is the elastic strain energy W_{e2}:

$$W_{e2} = -\frac{1}{2}F\triangle c \tag{10}$$

$$W_{e2} = -\frac{F^2 c}{2\,E\,b\,h} \tag{11}$$

where:

F is the peeling force of peeling bracts, [N]; E is the modulus of elasticity, [MPa]; θ is the peeling angle, [º]; b is the bract peeling width, [mm]; h is the bracts thickness, [mm]; R is the unit peeling energy, bract peeling energy consumption per unit area of bract peeling, [J].

According to the law of conservation of energy, the following equation is established:

$$-bcR + c(1-\cos\theta)F + \frac{F^2 c}{2Ebh} = 0 \tag{12}$$

By solving this equation, the formula for the bract peeling force F is obtained as shown in Eq. 13:

$$F = Ehb\left[\sqrt{(1-\cos\theta)^2 + \frac{2R}{Eh}} + \cos\theta - 1\right] \tag{13}$$

From Eq. (13), it is clear that the peeling force F during bract peeling depends on several factors such as the peeling angle θ, the bract peeling width b, the bract thickness h, the bract elastic modulus E, and the energy consumption R required for peeling each unit area.

Design of the key components

Scratching device

When the moisture content of corn cobs is high, the pores of the bracts become saturated with water (*Mandang et al., 2018*), causing the bract layers to stack tightly and wrap around the bare cob. As a result, the peeling rollers cannot effectively grip the bracts, leading to difficulties in the peeling process. Scratching the surface of the bracts can cause them to split at the point of contact, as shown in Fig.4d, allowing the peeling roller to better grip the bracts at the scratched location.

The scratching device as illustrated in Fig.7. The blade is welded to the bottom of the guide rail through the knife frame. The blade extends approximately 2 mm into the notch, ensuring it scratches a sufficient depth into the bracts without damaging the seeds. The operation principle is as follows: the cob passes through the semi-circular guide rail, which is set at a certain angle, and slides down the guide rail due to its gravity and the force from the pressing wheel (Fig.7a).

When the cob reaches the tip of the blade, the pressing wheel exerts both downward and forward forces on the cob, causing the cob to move over the blade (Fig.7b).

This action effectively scratches the bracts (Fig.7c). Furthermore, the semi-circular guide causes the corn cob to enter the peeling device in a vertical orientation, reducing the likelihood of clogging within the peeling device. This improvement enhances both the peeling efficiency and overall working performance.

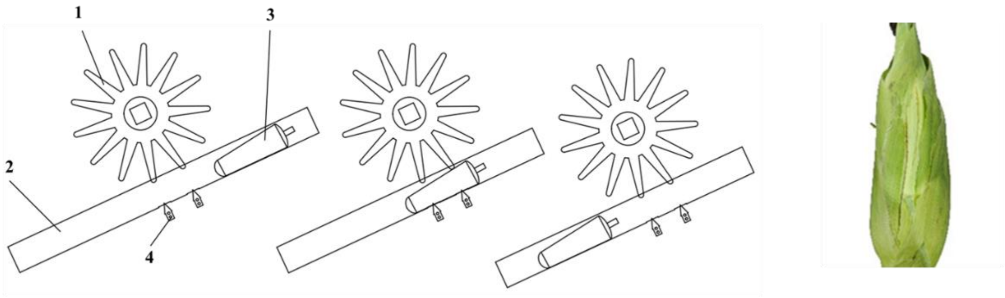

(a) Corn cob enter the inlet; (b) Lower bracts are scratched; (c) Corn cob complete with scratches. (d) Effect of bracts after scratching.

Fig. 4 – Schematic diagram of corn cob scratching and effect of bracts after scratching

1 - Pressing wheel; 2 - Semi-circular guide rail; 3 - Corn cob; 4 Blade.

Peeling device

The peeling device is illustrated in Fig.5. During the corn cob peeling process, the peeling roller maintains continuous frictional contact with the bracts, which is a critical mechanism underlying the device's operation *(Fu et al., 2020; Gorad et al., 2019)*. The device's configuration incorporates both high and low rollers, making it particularly well-suited for cobs with tightly wrapped bracts. The surface of the peeling roller is designed with both fish scale rollers and double spiral rollers. The fish scale rollers, positioned as the high rollers, exert friction on the bracts, effectively gripping them. The low rollers are equipped with double spiral rollers, whose helical pattern promotes the cob's continuous forward movement. Furthermore, the height difference between the high and low rollers creates varying friction torques on the cob. This torque disparity not only aids in correcting the cob's position but also induces rotational motion around its axis, thus increasing the number of contact points between the bracts and the peeling roller *(Yang et al., 2021)*.

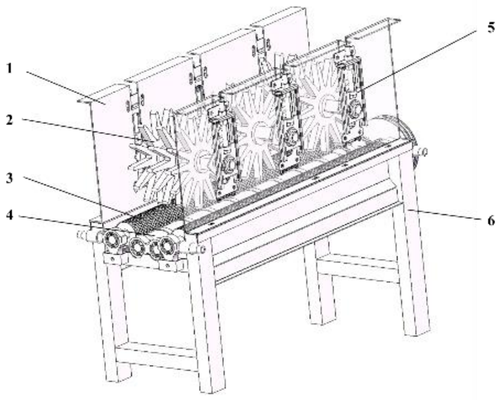

Fig. 5 – Peeling device

1 - Fixed plate; 2 - Pressing wheel; 3 - Fish scale roller; 4 - Spiral roller; 5 - Height-adjustable bearing seat; 6 - Frame.

High-speed camera experiment design

To verify the ability of the peeling roller to effectively grasp and remove bracts during the peeling of corn cobs with high moisture content, a high-speed camera peeling test platform was constructed, consisting of a high-speed camera and the peeling device (Fig.6). Before the test, the shooting frame rate set to 3000 frames/s and resolution set at 1920×1080. *(Zhu et al., 2015)*.

Fig. 6 – Test device

1 - Peeling device; 2 - Fill light; 3 - Computer; 4 - High-speed camera.

Peeling performance test design

The test samples used in this study were the Denghai 605 corn variety and were harvested in Liuyang City, Hunan Province, Chain. Samples exhibiting optimal cob length and undamaged bracts were selected, with moisture content maintained at approximately 35%. The test materials and device are illustrated in Fig. 7.

Fig. 7 – Test materials and device

Based on a theoretical mechanical analysis of the corn peeling process and preliminary pre-tests, three primary factors—peeling roller speed, pressing wheel speed, and the distance between the pressing wheel and peeling roller—were chosen for response surface test. Following JB/T11907-2014 standards, two evaluation metrics were selected: the bract peeling rate (Y_1) and the grain shedding rate (Y_2). The respective calculation formulas are given below:

$$Y_1=\left(1-\frac{n_b}{n}\right)\times 100\% \tag{14}$$

$$Y_2=\frac{G_s}{G+G_s}\times 100\% \tag{15}$$

where:

n is the total number of corn cobs of the measurement sample, [one]; n_b is the number of corn cobs without peeling bracts, [one]; G is the total mass of sample grains, [g]; G_s is the total mass of lost grains, [g].

Design of the one-way test

Based on both preliminary pre-tests and relevant research conducted by scholars domestically and internationally, the peeling roller speed was set within the range of 300~500 r·min^{-1}, the pressing wheel speed was set within the range of 40~120 r·min^{-1}, and the distance between the pressing wheel and peeling roller was set between 30 and 50 mm *(Li, 2023).* As detailed in Table 1.

Table 1

Single-factor test levels

Level	Factor		
	The peeling roller speed [r·min^{-1}]	The pressing wheel speed [r·min^{-1}]	The distance between the pressing wheel and the peeling roller [mm]
1	300	40	30
2	350	60	35
3	400	80	40
4	450	100	45
5	500	120	50

Response surface test

Based on the results of the one-way test, the following parameter ranges were selected: peeling roller speed of 300~400 r·min^{-1}, pressing wheel speed of 60~100 r·min^{-1}, and the distance between the pressing wheel and peeling roller set at 35~45 mm. The factor levels are presented in Table 2.

Table 2

Factor coding of peeling test

Encodings	Factor		
	Peeling roller speed [r·min^{-1}]	Pressing wheel speed [r·min^{-1}]	Distance between the pressing wheel and the peeling roller [mm]
-1	-1	-1	-1
0	0	0	0
1	1	1	1

RESULTS AND DISCUSSION

Results and analysis of the high-speed camera

Figure 8 presents the high-speed camera's capture of the cob bracts removal process post-scratching. Analysis of the high-speed footage revealed that the peeling process can be divided into two distinct stages: Firstly, due to the height difference between the high and low rollers, the friction torque acting on the cob varies, causing the cob to rotate around its axis. Simultaneously, the bracts' surface becomes puckered after being scratched. The pressing wheel intermittently applies pressure to the cob, which increases the friction between the peeling rollers and the scratched bracts. When this friction exceeds the bond between the layers of the bracts, the peeling rollers effectively grip the bracts (Fig. 8a–c). Secondly, once the peeling rollers grasp the bracts, they are continuously pulled. As the area of the bracts engaged between the two peeling rollers increases, the bracts break along the longitudinal veins, completing the peeling process (Fig. 8 d–f). Once the upper layer of bracts is peeled, the lower layers continue to be pulled by the combined forces of the peeling rollers and pressing wheel. Meanwhile, the cob continues to rotate around its axis, allowing each successive layer of bracts to be grasped and peeled until all the bracts are removed, as depicted in (Fig. 8 g–h). Thus, in the corn cob peeling process, increasing the friction between the peeling rollers and appropriately adjusting the difference in friction torque between the high and low rollers can facilitate the cob's rotation around its axis. This increases the contact time between the bracts and the peeling rollers, thereby improving the efficiency of bract removal.

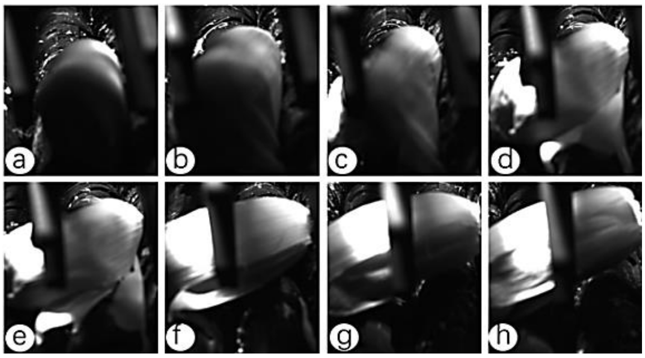

Fig. 8 – High-speed camera capture of bracts peeling process

Results and analysis of the one-way test

The results of the single-factor tests are presented in Fig. 9. As illustrated in Fig. 9, an increase in peeling roller speed, pressing wheel speed, and the distance between the pressing wheel and the peeling roller initially led to an increase in the bract peeling rate, followed by a subsequent decrease. In contrast, the grain shedding rate initially decreased and then increased. Specifically, when the peeling roller speed ranged from 300 to 400 r·min^{-1}, the maximum bract peeling rate reached 95%, and the minimum grain shedding rate was 1.45%. Similarly, when the pressing wheel speed varied between 60 and 100 r·min^{-1}, the maximum bract peeling rate increased to 96.67%, with a minimum grain shedding rate of 1.47%. When the distance between the pressing wheel and the peeling roller was adjusted to 35~45 mm, the maximum bract peeling rate was 95%, and the minimum grain shedding rate was 1.65%. Consequently, the optimal settings for the response surface test were determined to be a peeling roller speed of 300~400 r·min^{-1}, a pressing wheel speed of 60~100 r·min^{-1}, and a distance between the pressing wheel and the peeling roller of 35~45 mm.

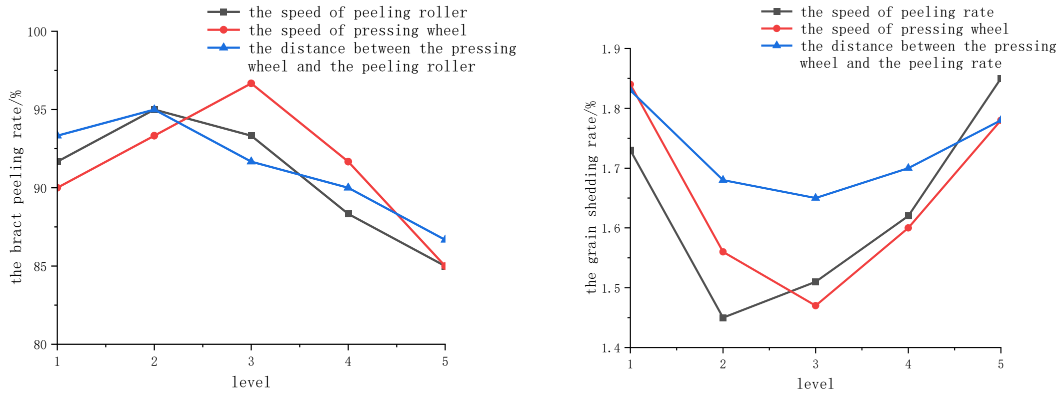

Fig. 9 – Single factor test results

Text results

Design-Expert 13 software was utilized for experimental design and data analysis, with the experimental design and results summarized in Table 3.

Table 3

Experiment scheme and results

Test number	Factor X_1	X_2	X_3	Y_1%	Y_2%
1	0	0	0	95	1.45
2	1	0	-1	93.33	1.71
3	0	0	0	93.33	1.39
4	-1	1	0	88.33	1.88
5	0	0	0	95	1.53
6	0	0	0	95	1.48
7	1	0	1	91.67	1.69
8	0	1	-1	93.33	1.65
9	0	-1	1	90	1.83
10	0	-1	-1	91.67	1.63
11	-1	0	-1	91.67	1.69
12	0	1	1	88.33	1.79
13	1	1	0	93.33	1.99
14	-1	0	1	86.67	2.05
15	1	-1	0	86.67	1.71
16	-1	-1	0	88.33	1.92
17	0	0	0	96.67	1.49

Significance analysis

The analysis of significance for the bract peeling rate (Y_1) and grain shedding rate (Y_2) is shown in Table 4. Both regression models for Y_1 and Y_2 were found to be statistically significant, with P-values less than 0.01. This indicates that the models effectively describe the relationship between the experimental factors and the response variables. Moreover, the regression equations were not found to be significantly out of fit, suggesting a strong quadratic relationship between the test parameters and the factors within the tested range. The coefficients of determination (R^2) for Y_1 and Y_2 were 0.9195 and 0.9558, respectively, demonstrating high consistency between the predicted and actual values. Based on the results, the regression terms X_3, X_1^2, and X_2^2 significantly influence Y_1 (P< 0.01). The interaction terms X_1, X_1X_2 and X_3^2 also showed a significant effect on Y_1 (0.01 < P < 0.05). Conversely, the regression terms X_2, X_1X_3, and X_2X_3 did not significantly affect Y_1 (P > 0.05). The corresponding regression equation for the bract peeling rate is provided in Eq. (16). For the grain shedding rate (Y_2), the regression terms X_3, X_1^2, and X_2^2 were found to have a very significant effect (P < 0.01). The interaction terms X_1, X_1X_2, X_1X_3, and X_3^2 were significantly associated with Y_2 (0.01 < P < 0.05). However, the terms X_2 and X_2X_3 had no significant impact on Y_2 (P > 0.05). The regression equation for the grain shedding rate is presented in Eq. (17).

$$Y_1=95+1.25X_1-1.67X_3+1.66X_1X_2-2.92X_1^2-2.92X_2^2-1.25X_3^2 \tag{16}$$

$$Y_2=1.47-0.055X_1+0.085X_3+0.08X_1X_2-0.095X_1X_3+0.2335X_1^2+0.1735X_2^2+0.0835X_3^2 \tag{17}$$

Table 4

Significance test result

Source of variation	Y_1 Sum of Squares	Degrees of freedom	F	P	Y_2 Sum of Squares	Degrees of freedom	F	P
Mold	143.03	9	8.89	0.0044	0.5736	9	16.82	0.0006
X_1	12.5	1	6.99	0.0332	0.0242	1	6.39	0.0394
X_2	5.53	1	3.09	0.1221	0.0060	1	1.60	0.2469
X_3	22.21	1	12.42	0.0097	0.0578	1	15.25	0.0059
X_1X_2	11.09	1	6.2	0.0416	0.0256	1	6.75	0.0355
X_1X_3	2.79	1	1.56	0.2519	0.0361	1	9.53	0.0177
X_2X_3	2.77	1	1.55	0.2531	0.0009	1	0.2375	0.6409
X_1^2	35.81	1	20.03	0.0029	0.2296	1	60.57	0.0001
X_2^2	35.87	1	20.06	0.0029	0.1267	1	33.44	0.0007
X_3^2	6.57	1	3.67	0.0969	0.0294	1	7.75	0.0272
Residual	12.52	7			0.0265	7		
Lost Proposal	6.94	3	1.66	0.3113	0.0157	3	1.92	0.2682
Pure error	5.58	4			0.0109	4		
Aggregate	155.54	16			0.6002	16		
R^2	0.9195				0.9558			

Response surface analysis

Based on the regression equations and response surface analysis (see Fig. 10), an interaction was observed between the peeling roller speed, the pressing wheel speed, and the distance between the pressing wheel and the peeling roller. As the peeling roller speed increased, the bract peeling rate initially increased and then decreased, with the maximum rate observed in the range of 340~360 r·min^{-1}. Similarly, the bract peeling rate increases and then decreases with increasing pressing wheel speed, reaching its maximum in the range of 70~85 r·min^{-1}. Moreover, as the distance between the pressing wheel and the peeling roller increases, the bract peeling rate initially increases slowly and then decreases, with the maximum rate observed between 37 and 41 mm. In summary, the optimal bract peeling rate for corn cobs with high moisture content occurs when the peeling roller speed is between 340 and 360 r·min^{-1}, the pressing wheel speed ranges from 70 to 85 r·min^{-1}, and the distance between the pressing wheel and the peeling roller lies between 37 and 41 mm.

Based on the regression equation and response surface analysis (Fig. 11), an interaction was observed between the peeling roller speed, the pressing wheel speed, and the distance between the pressing wheel and the peeling roller. As the peeling roller speed increased, grain shedding initially decreased and then increased, with the minimum shedding rate occurring in the range of 340~360 r·min^{-1}. Similarly, grain shedding decreased and then increased with an increase in pressing wheel speed, with the minimum rate observed between 75 and 85 r·min^{-1}. Furthermore, as the distance between the pressing wheel and the peeling roller increased, grain shedding decreased and then increased, with the minimum shedding rate occurring within the interval of 35~39 mm. In summary, the optimum peeling rate for corn cobs with high moisture content was achieved when the peeling roller speed was between 340 and 360 r·min^{-1}, the pressing wheel speed was between 75 and 85 r·min^{-1}, and the distance between the pressing wheel and the peeling roller was between 35 and 39 mm, simultaneously minimizing the grain shedding rate.

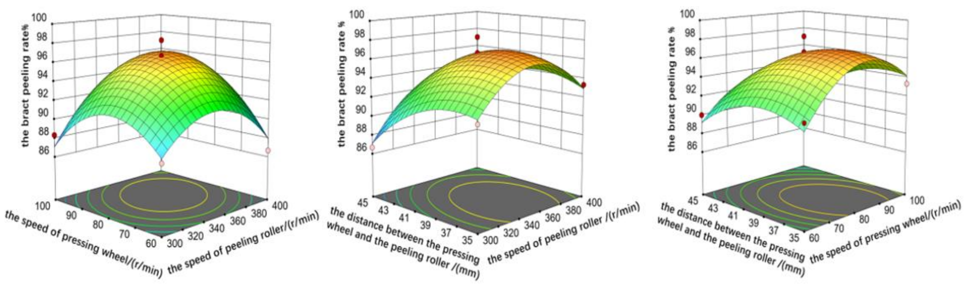

(a) $X_3 = 0$ (b) $X_2 = 0$ (c) $X_1 = 0$

Fig. 10 – Effect of factor interactions on bract peeling rate

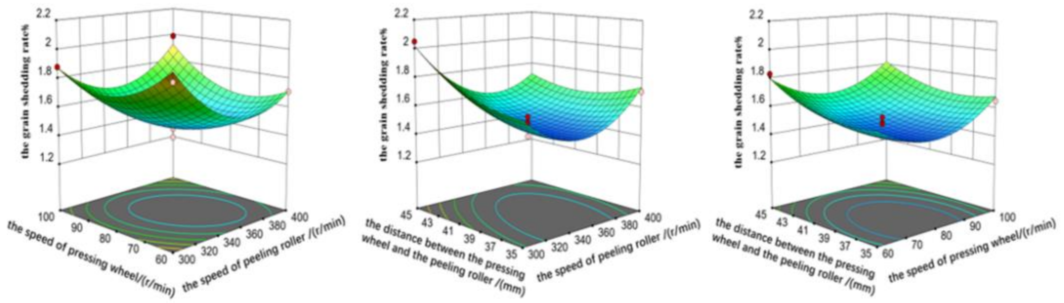

(a) $X_3 = 0$ (b) $X_2 = 0$ (c) $X_1 = 0$

Fig. 11 – Effect of factor interactions on grain shedding rate

Validation test

Using the optimization module of Design-Expert 13 software, the quadratic regression models for Y_1 and Y_2 are optimized and solved, with the objective function and constraints defined as follows:

$$\begin{Bmatrix} maxY_1 \\ minY_2 \\ 300r \cdot min^{-1} \leq X_1 \leq 400r \cdot min^{-1} \\ 60r \cdot min^{-1} \leq X_2 \leq 80r \cdot min^{-1} \\ 35mm \leq X_3 \leq 45mm \end{Bmatrix} \tag{18}$$

It led to the identification of the optimal parameter combination: peeling roller speed of 353.2 r·min^{-1}, pressing wheel speed of 81.42 r·min^{-1}, and a distance of 37.16 mm between the pressing wheel and the peeling roller. The bract peeling rate and grain shedding rate were found to be 95.67% and 1.45%, respectively.

The optimized test conditions were adjusted as follows: peeling roller speed of 353 r·min^{-1}, pressing wheel speed of 80 r·min^{-1}, and a distance between the pressing wheel and the peeling roller of 37 mm. To validate these conditions. Three repetitions were performed, resulting in an average bract peeling rate of 93.33% and an average grain shedding rate of 1.56%. These results, as presented in Table 5, fulfil the machine design specifications.

Table 5

Test validation results

Test number	Bract's peeling rate	Grain shedding rate
1	95%	1.55%
2	90%	1.59%
3	95%	1.54%
Average value	93.33%	1.56%

CONCLUSIONS

(1) A peeling device was designed to remove the skin through friction, following the initial scratching of the surface of the cob bracts. Additionally, the design of the scratching mechanism ensured that the surface of the cob bracts was scratched to a specific depth without damaging the seeds. The semi-circular guide rail was incorporated to position the corn cob vertically as it entered the peeling device.

(2) A peeling test platform, comprising a high-speed camera and the peeling device, was established to investigate the cob peeling process and verify that the peeling rollers can effectively grip the bracts at the points where the surface was scratched.

(3) Using Design-Expert 13 software to process the experimental data, the optimal parameter combination for the peeling device was identified as follows: peeling roller speed of 353.2 r·min^{-1}, pressing wheel speed of 81.42 r·min^{-1}, and a distance of 37.16 mm between the pressing wheel and the peeling roller. Under these conditions, the bract peeling rate was 95.67%, while the grain shedding rate was 1.45%. In the verification test, the bract peeling rate was 93.33%, the grain shedding rate was 1.56%, and the device met the design requirements.

ACKNOWLEDGEMENTS

This work is financially supported by the Hunan Provincial Natural Science Foundation Project (2024JJ6248), the open Fund of State Key Laboratory of Agricultural Equipment Technology (SKLAET-202406) and the Hunan Agriculture Research System (HARS-02)

REFERENCES

[1] Barnwal, P., Kadam D.M., Singh K.K. (2012). Influence of Moisture Content on Physical Properties of Maize. *International Agrophysics*, Vol. 26, pp. 331-334, Punjab/India.

[2] Chen Qingwen, Zhi Chen, Han Zengde, Hao Fuping,Cui Junwei, Wu Hongxin, Feng Xiaochuan. (2014). Analysis and Prospects of the Corn Husker of Corn Harvester in China (我国玉米收获机剥皮装置的现状分析及展望). *Journal of Agricultural Mechanization Research*, Vol. 36, pp. 257-260, Beijing/China.

[3] Chen Shun, Zhang Xinwei, Jiang Chunxia, Yi Kechuan, Wang Qingqing, Sha Xuemeng, Zhang Xiaolong. (2023). Experimental Study on the Peeling Fracture Effect of Fresh Corn Ear Based on High and Low Roller Peeling Equipment. *Agriculture*, Vol.13, pp.8, Chuzhou/China.

[4] Fu Jun, Yuan Haikuo, Zhao Rongqiang, Chen Zhi, Ren Luquan. (2020). Peeling Damage Recognition Method for Corn Ear Harvest Using RGB Image. *Applied Sciences*, Vol.10, pp.10, Changchun/China.

[5] Kendall K. (1975). Thin-film peeling-the elastic term [J]. *Journal of Physics D Applied Physics*, Vol. 8, pp.1449, Ibaraki/Japan.

[6] Li Zhenye, Fu Jun, Luo Xiwen, Fu Qiankun,Chen Zhi, Ren Luquan. (2024). Determination of Friction Characteristics of Corn Ears at Varying Factors in Mechanical Peeling. J*ournal of Food Process Engineering*, Vol. 47, pp. e14764, Jilin/China.

[7] Liu J.J., Ye W., Zhang Z.H., Yu Z.L., Ding H.Y., Zhang C., Liu S. (2020). Vein distribution on the deformation behavior and fracture mechanisms of typical plant leaves by quasi in situ tensile test under a digital microscope. *Appl.Bionics Biomech*, Vol. 49, pp. 1643-1652, Huai'an/China.

[8] Li Zhenye, Fu Jun, Luo Xiwen. (2021). Tensile Properties and Fracture Mechanisms of Corn Bract for Corn Peeling Device Design. *Agriculture*. Vol. 11, pp. 796, Jilin/China.

[9] Liu Lei, Du Yuefeng, Li Xiao, Liu Lihan, Zhang Yan'an, Fan Y. (2022). Analysis and Experiment on Kernel Loss of Seed Corn during Peeling Based on DEM (基于离散元法的种子玉米剥皮过程籽粒损失分析与试验). *Transactions of the Chinese Society for Agricultural Machinery*. Vol. 53, pp. 28-38, Beijin/China.

[10] Li Zhenye. (2023). *Research on key technologies and intelligent recognition for low-damaged-high-stripping peeling of corn ear harvester (玉米果穗收获机低损高净剥皮关键技术与智能识别研究)* (PhD dissertation, Jilin University, Jilin/China).

[11] Mandang T., Sinambela R., Pandianuraga N. (2018). Physical and mechanical characteristics of oil palm leaf and fruits bunch stalks for bio-mulching [J]. *IOP Conference Series: Earth and Environmental Science*, Vol. 196, pp. 012015. 012015, Pertanian Bogor/ Indonesia

[12] Plett S. (1994). Corn kernel breakage as a function of grain moisture at harvest in a prairie environment [J]. *Canadian Journal of Plant Science*, Vol. 74, pp. 543-544, Manitoba/Canada.

[13] Rivlin R. (1977). *The Effective Work of Adhesion* [M]. New York: Collected Papers of R.S. Rivlin. Springer New York. pp.2611-2614. New York/ Britain

[14] Shirly. (2015). Kubota 4YZB-3(PRO-1408Y) Self-propelled Corn Harvester. *Agricultural machinery*. Vol. 18, pp. 28.

[15] Xie Fuxiang, Song Jian, Huo Hongpeng, Huo Xinxin. (2018). Experiment and Mechanical Characteristics on Bract Peeling of Corn Harvester (玉米苞叶力学性能与剥离试验). *Agricultural Mechanization Research*, Vol. 40, pp. 129-133, Qingdao/China.

[16] Yang Ke, Jiang Chun-Xia, Zhang Wei, Zhang Dong-Mei, Liu En-Ke, & Guang-Gian, Z. (2023). Effects of Different Harvesting Time on the Mechanical Harvest Quality and Yield of Maize Grains (不同收获期对玉米子粒机械收获质量及产量的影响). *Journal of Maize Sciences*, Vol. 31, pp. 88-94, Taiyuan/China.

[17] Yang Fan, Du Yuefeng, Fu Qiufeng, Li Xiaoyu, Zhu Zhongxiang. (2021). Design and testing of seed maize ear peeling roller based on Hertz theory. *Biosystems Engineering*, Vol. 202, pp. 165-178, Beijing/China.

[18] Zhao Yiming, Dai Fei, Shi Ruijie, Chen Junzhi, Xin Shanglong, Zhao Wuyun, Fengwei, Z. (2024). Design and Experiment of Self-propelled Seed Corn Combine Harvester (自走式制种玉米联合收获机设计与试验). *Transactions of the Chinese Society for Agricultural Machinery*. Vol. 55, pp. 121-134, Lanzhou/China.

[19] Zhao Chun Hua, Zhao Tao, Long H.B. (2012). Design and Experimental Study of the Multi-Function Corn Peeling Machine with Analysis of Segmented Metal Construction Materials. *Advanced Materials Research*, Vol. 600, pp. 144-147, Lanzhou/China.

[20] Zhu Zhongxiang, Yue Xiaowei, Du Yuefeng. (2015). Dynamic simulation and high-speed photography experiment on corn-ear husking (玉米果穗剥皮的运动仿真与高速摄像试验). *Transactions of the Chinese Society of Agricultural Engineering*. Vol. 31, pp. 42-48, Beijing/China.